03

Experimental and computational microfluidics for studying the characteristics of oil displacement in porous media

© I.Ch. Garifullin,[1] S.Y. Fazletdinov,[2,3] Yu.A. Pityuk,[2] E.S. Batyrshin[2]

[1] Ufa University of Science and Technology,
450077 Ufa, Russia
[2] LLC „RN-BashNIPIneft" (GS of PJSC Rosneft „Oil Company"),
450103 Ufa, Russia
[3] Ufa Federal Research Center of the Russian Academy of Sciences,
450054 Ufa, Russia
e-mail: GarifullinISh@yandex.ru, spartak.fazlet@gmail.com

Received January 22, 2025
Revised June 30, 2025
Accepted July 18, 2025

A microfluidic approach to efficient oil recovery from porous media is presented. The paper focuses on enhanced oil recovery methods using surfactants. The advantages of the proposed method using microfluidic chips compared to traditional core filtration experiments are demonstrated. A combined experimental and numerical approach is proposed for evaluating the efficiency of various displacing agents. The capabilities and limitations of freely available computational packages for porous network modeling are discussed. Experimental results are compared with numerical simulations. Experimental results are presented demonstrating the influence of wettability on oil displacement efficiency. The effectiveness of surfactant solutions in reducing residual oil saturation is demonstrated. The presented approach is considered a promising option for rapid screening of agents affecting productive formations.

Keywords: enhanced oil recovery, surfactants flooding, microemulsion, pore network, microfluidic chip.

DOI: 10.61011/TP.2026.01.62838.8-25

Introduction

Effective extraction of oil from porous media is a key task of oil and gas industry. There are several successively used methods of deposit development. The primary method is based on hydrocarbon production by natural energy of a stratum, which provides their movement to production boreholes. The secondary method involves pumping water into pressure boreholes. The primary and secondary methods can produce about 30 % of the total oil reserves [1]. The residual oil is held by capillary forces or remains in blind pores of a reservoir. Mobilization of this oil requires application of various methods of enhanced oil recovery (EOR). Flooding using surfactant-based solutions is one of these methods [2]. Surfactant flooding provides additional oil displacement due to action of several mechanisms: reduction of interphase tension [3], variation of wettability [4] and emulsification [5]. In addition, application of specially selected surfactant compositions makes it possible to achieve formation of a microemulsion, which is accompanied by reduction of interphase tension by several orders [6] and significantly enhances a surfactant application effect. At the same time, because of uniqueness of an oil composition and stratum conditions these compositions shall be individually selected for each object. Traditionally, selection of the optimal surfactant composition is based on performing some laboratory tests, which result in determination of physical-chemical properties of the compositions, interphase tension, compatibility of displacement agents with stratum fluids as well as equilibrium diagrams of a three-component surfactant/oil/water system. Composition ranking is followed by estimating displacement coefficients as a result of filtration studies on bulk models [7] or a core [1]. The results of the core tests are crucial when selecting the surfactant compositions, but labor intensity and long duration of these studies make selection of the displacement agents an extremely costly and long procedure. Additionally, when displacing in the porous medium it is impossible to visualize processes in a scale of separate pores, thereby prevents from differentiating mechanisms that provide additional oil production. For the said reasons, a tool for rapid and effective screening of the displacement agents is more and more often is considered to be microfluidic systems, whose main idea is related to performing the filtration tests on microfluidic chips that are rock analogues [8–11].This approach makes it possible to qualitatively rank various compositions by a degree of efficiency at preliminary stages for selecting the displacement agents. The microfluidic chips are optically transparent devices, which include single microchannels or their networks. The main advantages of the chip-based experiments are due to visualizing a multi-phase flux of fluids in a pore space. It allows analyzing a relation of integral characteristics of the multi-phase flux with the pore-scale processes.

An important tool supplementing the experiments is numerical simulation, which allows performing multivariant

calculations for the various displacement agents in several times faster than the laboratory studies, while keeping important physical and geometrical properties of a core pore space. At the same time, preliminary numerical simulation allows selecting an optimal design of the microfluidic chip taking into account available limitations when solving a specific problem.

As compared to a Boltzmann lattice equation method [12,13] and a particle method [14,15], porous network modeling methods [16,17] are more attractive, since they take less time and are less demanding to computational resources due to representing the pore space as a network of pores and channels. At the same time, this method can take into account physical-chemical properties of a displacing agent and a rock, such as its density, viscosity and surface tension between the fluids, a wetting angle, etc. This, in turn, enables estimating the influence of these properties on a process of oil displacement by various agents as well as selecting optimal parameters of the surfactant solutions, which provide maximum displacement of oil from the pore network.

The present study provides numerical and experimental investigation of processes of heptane displacement by various displacing agents and, particularly, shows the influence of wettability on a value of a displacement coefficient. The numerical approach was tested based on the experimental data. Novelty of the present study includes the developed approach and new experimental data that confirm that application of a specially selected solution increases efficiency of oil displacement.

1. Experimental technique and materials

The microfluidic chips were manufactured using method of photolithography and chemical etching. The chips are two glued glass plates, wherein one of them has the microchannel network formed and the other has holes for supply and removing fluids made. A procedure of microstructure formation and plate gluing is described in detail in the study [18]. The pore space of the chips was a pore network structure — a system of cylindrical pores interconnected by channels shaped as rectangular parallelepipeds. A structure of the channels in the plane of the microfluidic chip is shown in Fig. 1, *a*. The pores are distributed in nodes of the rectangular lattice and interconnected by the straight channels. The pore network is connected to a network of auxiliary channels, which is designed for supplying and removing the fluid flux. Fig. 1, *b* shows a three-dimensional fragment of the pore network, which provides the most detailed representation of the structure of the pore space of the chip. A diameter of all the pores was $80\,\mu$m, while a width of the channels was randomly pre-defined equally likely within a range from 25 to $55\,\mu$m. A height of all the pores and the channels was the same to be $6\,\mu$m. Porosity and permeability of the model were 53 % and $4.1 \cdot 10^{-14}\,\text{m}^2$,

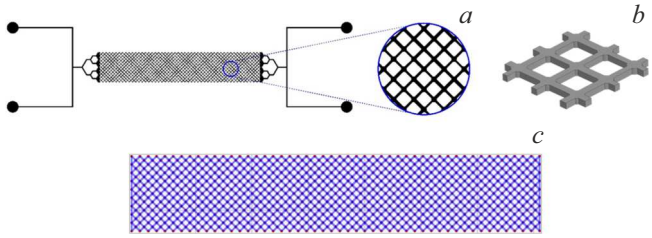


Figure 1. Structure of the pore space of the chip: *a* — plan view in a glass plate's plane; *b* — three-dimensional visualization; *c* — plan view of the numerical porous network model.

respectively. A material of the microfluidic chips (glass) allowed their multiple use. For this purpose, after each experiment, the pore space of the chips was successively flushed by a mixture of toluene (Khimreaktivsnab, Russia) and isopropanol (Khimreaktivsnab, Russia) in a ratio 2 : 1 deionized water and purged with air. Flushing was followed by drying the chips in a heating cabinet (Ulab, Russia) at the temperature of 120 °C.

N-heptane was used as a hydrocarbon phase in the experiments (LLC „Proton", Russia). The displacing solutions (displacement agents) were prepared by using: an anion surfactant — sodium dodecyl sulfate (Sigma-Aldrich, USA), n-butanol (Khimreaktivsnab, Russia), sodium chloride (JSC „MZKhR", Russia). Table shows the displacement agents used in the study. The brine was used for simulating a basic option of oil displacement by pumping in water. The surfactant solution was used as a standard EOR agent designed to increase production by reducing interphase tension. The latter solution was a solution of two mutually complementing surfactants (surfactant/cosurfactant). Using this solution with a correctly selected concentration and a component content ratio makes it possible to form a microemulsion at a displacement front, thereby obtaining additional oil production [19]. Aqueous solutions were dyed by adding bromophenol blue (Khimreaktivsnab, Russia) in a mass concentration of 0.2 % for contrasting water and hydrocarbon phases during displacement. The experiments were performed on the chips with various wettability. For some chips, an initial hydrophilic surface of the pore space was modified into a hydrophobic one using a two-percent solution of dimethylchlorosilane (ABCR, Germany) in toluene [20].

The microfluidic installation (Fig. 2) was assembled on a table of an optical microscope Olympus IX-71 (Olympus, Japan) coupled with the chamber Lumenera Infinity 2 (Lumenera, USA). The microfluidic chip was fixed in a special holder that provided connection to fluid sources and thermal stabilization. All the experiments were carried out at the temperature of 30 °C. A fluid flow in the chip was controlled by a value of applied pressure drop and the pressure was pre-defined by means of a pressure controller (Parker, USA). During displacement, images of the pore network were recorded with resolution of 2448x2048 dots.

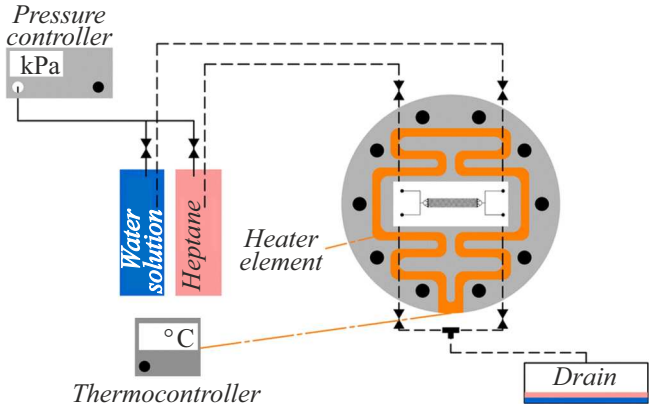


Figure 2. Schematic diagram of the experimental setup for the microfluidic studies.

Displacement agents

Displacement agent	Composition
Brine	4 weight% -solution of sodium chloride (NaCl) in water
Surfactant solution	5 weight% -solution of sodium dodecyl sulfate (SDS) in the salt solution
Surfactant/cosurfactant solution	5 weight%-solution of the SDS/butanol mixture (the weight ratio of SDS : butanol = 1 : 2) in the brine

Since the entire chip structure was unfit in a microscope vision field, the complete images of the pore space of the chips were stitched from separate fragments using the Hugin software [21]. The images were segmented for estimating fluid saturation as well as wetting contact angles were estimated (Fig. 2, *b*) using the ImageJ software [22]. Fig. 2, *c* shows segmentation of the image: the white domains correspond to heptane and the black domains correspond to the displacing agent. A portion of white pixels to a total number of pixels occupied by the pore network determines a residual portion of heptane in the pore network.

2. Numerical simulation methods

Two packages for pore network modeling were used for numerical simulation: OpenPNM [16] and PNFlow [17]. In the pore network models, calculation nodes are pores that are connected by a channel. A flux between these two pores is considered to be an isothermal incompressible flow of a viscous liquid in a pipe, which can be described by any number of analytical solution in a dependence on a geometry of the pipe (channel). In case of a cylindrical channel, the Hagen-Poiseuille equation is used. For a quasistatic approximation, the system of equations is written as follows:

$$Q_{ij} = g_{ij}(P_i - P_j), \quad (1)$$

where Qij is a flowrate between the pores i and j; Pi and Pj are pressures in the pores i and j, respectively; gij is hydraulic conductivity of the channel between the pores i and j, which depends on a length, area of a channel cross section and liquid viscosity.

A mass conservation equation in the pore network model for internal pores is described by the Kirchhoff law. The pressure field in the entire network can be calculated by applying the mass conservation equation to all the pores with respective boundary conditions that are pre-defined by pressure values in inlet and outlet pores. A capillary pressure in the channels is calculated depending on its form [23]. Calculation of the pressure field is followed by finding the flowrate in the pore network, which is used for determining absolute permeability of the pore network model according to the Darcy's law.

First of all, it was simulated in the OpenPNM software package, in which some limitations were discovered. The first one of them is that cylindrical channels are considered and, therefore, elements of the pore network can be fully saturated with only one phase. It does not allow simulating capture of one of the phases in angles and, consequently, angular flows that occur in real displacement processes in the porous media. Besides, only one static contact angle can be pre-defined, which does not allow simulating random processes in displacement, which occur in filtration in the porous media and are observed in the experiments on the microfluidic chips.

Due to the discovered limitations of the OpenPNM software package we considered the second package for pore network simulation PNFlow, which allows taking into account partial filling of the elements of the pore network model with a various geometry. Besides, the PNFlow allows pre-defining random distribution of the contact angles, which is observed in the experiments on the chips. The PNFlow pre-defines both static and dynamic contact angles with various models. The static contact angles can be pre-defined both by an equilibrium angle for all the elements and the Weibull distribution [24]. For the dynamic contact angles, one can pre-define a constant value or as a uniform distribution. In addition, receding and advancing contact angles can be pre-defined by classes of the Morrow angles [25].

3. Experimental results

Initial and changed wettability of the microchannel surface was controlled by a sessile droplet technique. Fig. 3 shows water droplets on the glass plate surface, which were used for chip manufacturing. A wetting angle of the unmachined initial surface at a „glass-water-air" interface was 24°, so was that of the machined surface 91°. Thus, surface machining made it possible to change initial

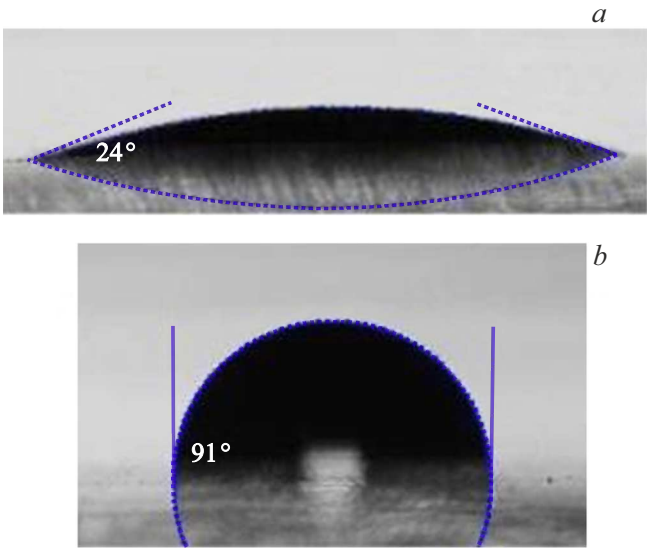


Figure 3. Contact angles of glass surface wetting: *a* — the initial surface; *b* — the machined surface.

hydrophilic wettability of the plate surface into hydrophobic one.

Characteristics of heptane displacement by various solutions were determined as a result of filtration experiments. The pore space of the microfluidic chip was pre-filled with heptane to a state of hundred-percent saturation and then the displacing agent was pumped in at the constant pressure drop. The displacement coefficient was determined as a relative change of saturation of the pore network with the hydrocarbon phase as a result of displacement. Since the height of the pores and channels of the chip is a magnitude that is constant for all portions of the pore network, the phase volume ratio is equal to a ratio of areas of image fragments, which are occupied by the water and hydrocarbon phases. The areas of the image areas that correspond to the various phases were easily determined, since the water phase was specially dyed for contrasting.

Initially, efficiency of the solution was estimated by performing experiments of hydrocarbon displacement by the brine under conditions of various chip wettability. These experiments included simulation of the basic diagram of flooding during deposit development. Fig. 4, *a* shows the typical pattern of displacement for the hydrophilic pore network structure. The typical flowrate and the displacement time were 0.04 μl/min and 370 s, respectively. In this case, a displacement front was almost piston-like and is clearly localized. In the hydrophilic chip, the displacing agent is a wetting liquid, therefore, the capillary forces facilitate displacement. The wetting contact angles at the „glass-displacing liquid-heptane“ interface varied within the range 20-40° (Fig. 4, *b*). The pore network image was segmented after displacement (Fig. 4, *c*) to provide estimation of the hydrocarbon phase displacement coefficient of 92 %.

The case of the hydrophobic chip exhibits a displacement pattern caused by an effect of the capillary forces (Fig. 5, *a*) that prevent heptane displacement. The typical flowrate and the displacement time were 0.03 μl/min and 450 s, respectively. The wetting contact angles at the „glass-displacing liquid-heptane“ interface are 108-143° (Fig. 5, *b*). This case exhibits large clusters of an immovable hydrocarbon phase, which are held by the capillary forces. As a result, the displacement coefficient was 80 %, which is noticeably smaller than the value for the case of the hydrophilic chip.

The experiments with application of the surfactant solutions were performed on the hydrophobic models. Fig. 6, *a* shows the typical patter of heptane displacement with the surfactant solution. Application of the surfactant makes it possible to reduce interphase tension at the „displacing liquid-heptane“ interface and, consequently, to reduce the capillary forces that prevent a flow of the displacing liquid. The typical flowrate and the displacement time were 0.18 μl/min and 90 s, respectively. These changes lead to leveling of the displacement front and make it possible to increase a relative portion of the pore network,

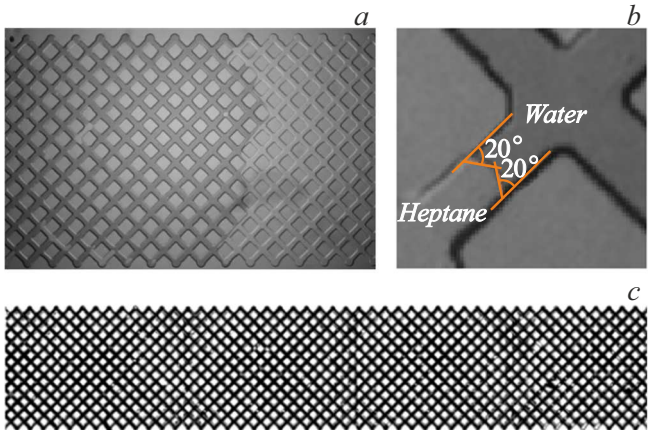


Figure 4. Hydrocarbon displacement by the brine in the hydrophilic model: *a* — a typical displacement pattern; *b* — a wetting contact angle; *c* — a fluid distribution. The bright domains mean heptane, the dark domains mean water.

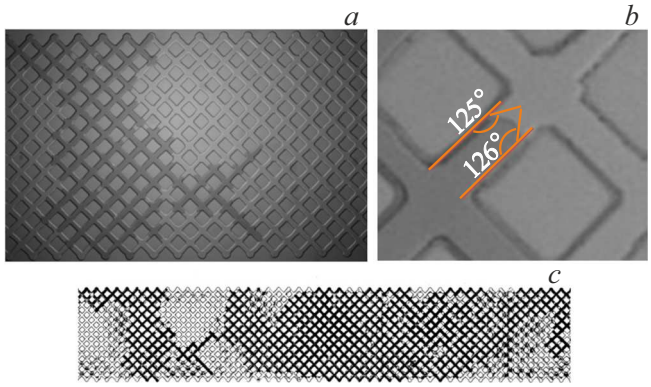


Figure 5. Hydrocarbon displacement by the brine in the hydrophobic model: *a* — a typical displacement pattern; *b* — a wetting contact angle; *c* — a fluid distribution. The bright domains mean heptane, the dark domains mean water.

which is involved in the filtration process. In this case, the contact angles varied within the range 133-151° (Fig. 6, *b*). An increase of drain coverage allowed reducing residual oil saturation and increasing the heptane displacement coefficient to 88 % (Fig. 6, *c*).

A special case of surfactant flooding is microemulsion flooding, when the surfactant composition is selected in such a way that a microemulsion phase is formed where the displacing agent contacts oil. Formation of the microemulsion is accompanied by reduction of interphase tension by several orders, thereby enabling additional extraction of oil. It was this surfactant/cosurfactant composition capable of forming the microemulsion when mixed with heptane that was used in the last series of the experiments (Fig. 7). During solution pumping, a piston displacement front is observed, but unlike simple surfactant flooding, „smearing" of the interface between the displacing agent and the hydrocarbon is observed over time (Fig. 7, *b*). A transition from the displacing agent (the dark domains) to the hydrocarbon (the bright domains) becomes smeared at the images (halftones are observed) without an interphase interface clearly localized in space. The said process of mutual dissolution of the water and hydrocarbon phases becomes possilbe due to a process of solubilization with formation of the microemulsion [26]. Absence of a pronounced interface between the phases is effectively expressed in reduction of interphase tension by several orders. The typical flowrate and the displacement time were 0.15 μl/min and 100 s, respectively. Displacement was followed by measuring the wetting contact angles at the „glass-displacement solution-heptane" interface, which were 124-129°. In this case, ultra-low values of the interphase tension coefficient made it possible to increase the displacement coefficient to 95.1 % (Fig. 7, *c*).

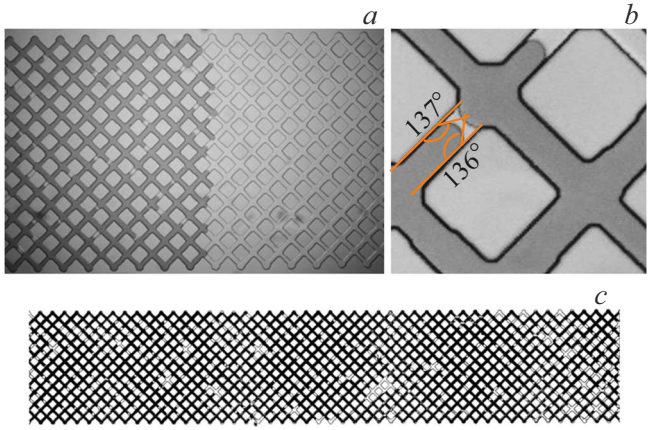


Figure 6. Hydrocarbon displacement by the surfactant solution in the hydrophobic model: *a* — a typical displacement pattern; *b* — a wetting contact angle; *c* — a fluid distribution. The bright domains mean heptane, the dark domains mean water.

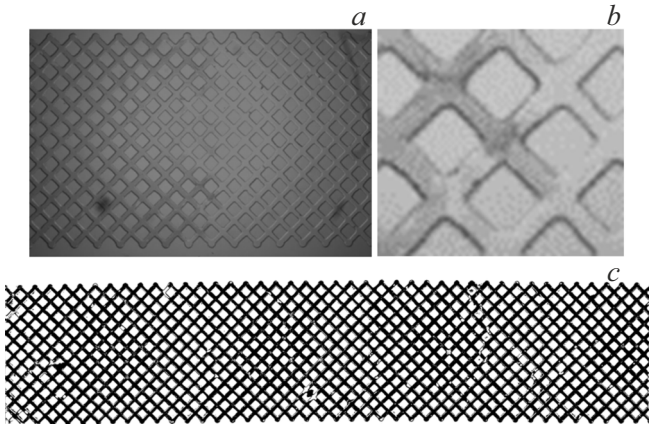


Figure 7. Hydrocarbon displacement by the surfactant/cosurfactant solution in the hydrophobic model: *a* — a typical displacement pattern; *b* — a wetting contact angle; *c* — a fluid distribution. The bright domains mean heptane, the dark domains mean water.

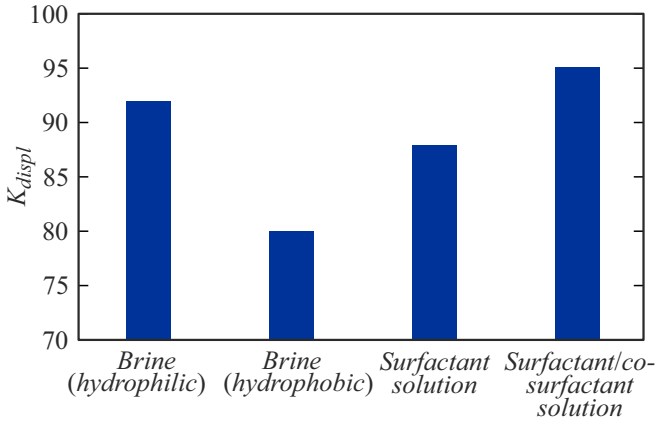


Figure 8. Comparison of efficiency of heptane displacement by the various agents in the hydrophobic model.

Comparison of efficiency of displacement by the various agents, which is shown in Fig. 8, shows the highest efficiency for the case of flooding using the solution capable of formation of the microemulsion. The showed experimental method allows detailing an effect of the displacement mechanisms in the scale of separate pores during surfactant flooding and can be used for selecting the optimal composition of the agent with surfactant addition for conditions of a specific deposit site. This technology of screening of the surfactant-containing agents using the microfluidic chips can be effectively used for large-scale preliminary tests in order to select candidates for studies on a real core.

4. Comparison of the numerical simulation results with the experimental data

The pore network model for numerical simulation is generated based on the experimental microfluidic chip

(Fig. 1, *b*) with application of the pnextract software package [13]. The total length of the generated model was 14 mm, and its width was 3 mm. Initially, the model was fully filled with heptane with viscosity of 3.86 10-4 Pa s, thereby corresponding to an experimental value of viscosity, which was obtained at the temperature of 30°C (the temperature of the laboratory studies). On the left, water with viscosity of 10-3 Pa s was supplied into the inlet pores. We have considered a case of displacement by salt water with the surface tension coefficient of 0.05 N/m and a hydrophobic surface with the dynamic contact angle within the range from 108 to 143° according to the experimental data. In the OpenPNM software package, the same surface tension coefficient and the contact angle of 130° was pre-defined in the numerical model. As a result, the heptane displacement coefficient was 79.4 %, thereby well agreeing with the experimental data, in which the heptane displacement coefficient was 80 %. Fig. 9, *a* shows a typical displacement pattern obtained as a result of numerical simulation in OpenPNM. It should be noted that despite well agreement of the heptane displacement coefficient the pores, which still have heptane after displacement, do not correspond to the experiment on the chips, where each experiment exhibits heptane capture in various pores while preserving the portion of displaced heptane at the same time. It is explained by prevalence of the capillary forces

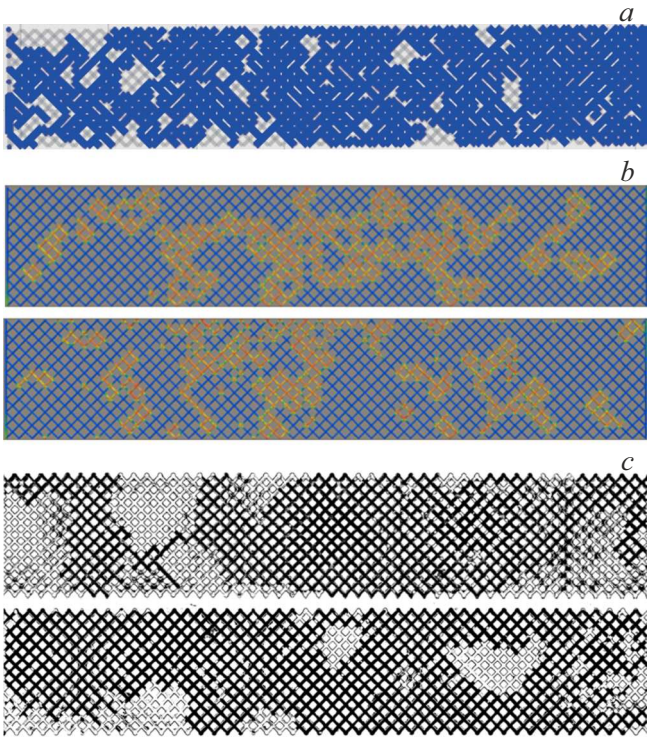


Figure 9. Comparison of the results of heptane displacement by salt water in the pore network model using OpenPNM (*a*), PNFlow (*b*) and in the experiment (*c*). In the first case $K_{displ} = 79.4\,\%$, when using PNFlow the result is identical to the experiment — $K_{displ} \approx 80\,\%$.

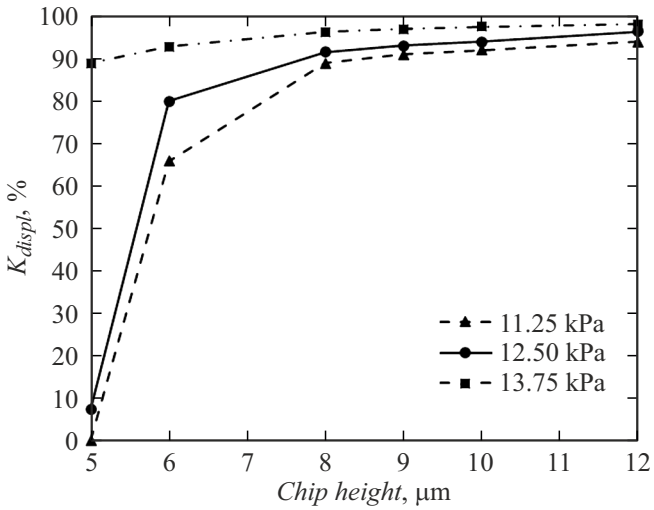


Figure 10. Variation of the heptane displacement coefficient in the pore network model in a dependence on the chip height at the various pressure drops.

that are significantly affected by the dynamic contact angles which are a random magnitude.

It was followed by calculating heptane displacement with salt water, but using the PNFlow software package. In the model, the static angles were pre-defined as a Weibull distribution within the range 108-143°, thereby corresponding to the experimental data. The dynamic contact angles were pre-defined by the MorrowIII class, which determines the receding and advancing angles based on the static one. This pre-definition of the static contact angle and the dynamic contact angles in the element of the pore network model in each calculation resulted in capturing different channels and pores (Fig. 9, *b*), thereby corresponding to displacement patterns observed during multiple performance of the experiments on the chip (Fig. 9, *c*). Launching a series of the calculations was followed by obtaining an average heptane displacement coefficient of 80 %, thereby corresponding to the experimentally-obtained displacement coefficient. It also included analysis of variation of the hydrocarbon-phase displacement coefficient in a dependence on the chip height at the various values of the pressure drop (Fig. 10). It is clear from the figure that with an increase of the chip height the heptane displacement coefficient increases. This fact is due to reduction of hydraulic resistance of the channels in the pore network model and, respectively, reduction of the capillary forced directed against the flow of the displacement agent. Besides, we note that with an increase of the pressure drop the portion of captured heptane decreases. But for the height of more than 8 μm the influence of the pressure drop does not significantly affect the displacement process, since a dominant role is beginningly played by a contribution by viscous forces, whose predominance results in the fact that almost the entire heptane is displaced from the pore network at slight pressure drops. It should be also noted that the pressure drop of 11.25 kPa in the chip of the height of 5 μm

is not enough to overcome the capillary forces and to start displacement. Thus, numerical simulation can be used for designing the microfluidic chip and selecting experimental conditions.

Thus, the PNFlow software package made it possible to simulate the displacement process in the pore network models, which is observed in the experiment on the chips, and can be used for developing the technologies of screening of the surfactant agents based on the microfluidic chips, including for preparing a design of the chip geometry.

Conclusion

Within the framework of the study, we have manufactured and tested an experimental platform using the microfluidic chips for studying the displacement processes in the porous media.

We have experimentally studied the process of the displacement of hydrocarbons as exemplified by n-heptane by the various displacement agents in the hydrophilic and hydrophobic microfluidic chips.

The experiments of displacement on the hydrophobic microfluidic chips by the various agents (the brine, the surfactant solution, the surfactant/cosurfactant solution) showed that the highest efficiency belongs to solutions that were capable of forming the microemulsion phase when contacting the hydrocarbons.

The proposed approach is a suitable testing platform for studying the displacement processes because it is possible to visualize and analyze the liquid behavior in the pore scale.

We have obtained the good agreement of the results of numerical simulation in the pore network simulation packages OpenPNM and PNFlow with the experimental data. It is shown that application of PNFlow better describes the experimental data.

The obtained results are practically important for developing the microfluidic screening technology for selecting the effective oil displacement agents, which in turn can affect an oil extraction industry of the economics in terms of developing innovative technologies of enhanced oil recovery.

Funding

This study was supported by grant №. 21-79-10212 from the Russian Science Foundation.

Conflict of interest

The authors declare that they have no conflict of interest.

References

[1] M. Fani, P. Pourafshary, P. Mostaghimi, N. Mosavat. Fuel, **315**, 123225 (2022).
[2] H. Imuetinyan, A. Augustine, A. Gbadamosi, R. Junin. Arabian J. Geosci., **15** (3), 226 (2022).
[3] X. Deng, Sh. Patil, M.Sh. Kamal, M. Mahmoud, A. Sultan, T. Saikia. Energy Fuels, **36** (14), 7391 (2022).
[4] G. Cheraghian, S. Rostami, M. Afrand. Processes, **8** (9), 1073 (2020).
[5] X. Zhao, F. Zhan, G. Liao, W. Liu, X. Su, Y. Feng. J. Colloid Interface Sci., **620**, 465 (2022).
[6] J. Pereira, A. Costa, N. Foios. Fuel, **134**, 196 (2014).
[7] O. Massarweh, A.S. Abushaikha. Geoenergy Sci. Eng., **221**, 211400 (2023).
[8] S. Gogoi, S.B. Gogoi. J. Petroleum Exploration Production Technol., **9**, 2263 (2019).
[9] L. Hao, P. Cheng. Intern. J. Heat Mass Transfer, **53** (9), 1908 (2010).
[10] M. Pryazhnikov, A. Pryazhnikov, A. Skorobogatova, A. Minakov, Y. Ivleva. Micromachines, **14** (6), 1137 (2023).
[11] D.I. Pereponov, A. Shcherbakova, V.V. Kazaku, M.E. Gadzhiev, M.A. Tarkhov, E.D. Shilov, A.N. Cheremisin. Vestnik neftegazovoi otrasli Kazakhstana, **5** (1), 57 (2023) (in Russian).
[12] M. Zhang, G. Ye, K.V. Breugel. Computational Mater. Sci., **68**, 142 (2013).
[13] A.M. Tartakovsky, P. Meakin. Adv. Water Resources, **29** (10), 1464 (2006).
[14] Y. Zhu, P.J. Fox. J. Computational Phys., **182** (2), 622 (2002).
[15] A.Q. Raeini, B. Bijeljic, M. Blunt. Phys. Rev. E, **96**, 013312 (2017).
[16] J. Gostick, M. Aghighi, J. Hinebaugh, Th.G. Tranter, M. Hoeh, H. Day, M.H. Sharqawy, B. Spellacy, A. Bazylak, A.D. Burns, W. Lehnert, A. Putz. Computing Sci. Eng., **18** (4), 60 (2016).
[17] P.N. Valvatne, M.J. Blunt. Water Resources Res., **40**, W07406 (2004).
[18] I.Sh. Garifullin, O.A. Solnyshkina, E.S. Batyrshin. Pribory i tekhnika eksperimenta, **5**, 187 (2024) (in Russian).
[19] J. Van Nieuwkoop, G. Snoei. J. Colloid Interface Sci., **103** (2), 400 (1985).
[20] H. Emami Meybodi, R. Kharrat, X. Wang. Transport in Porous Media, **89**, 97 (2011).
[21] Hugin [website]. Panorama photo stitcher. URL: https://hugin.sourceforge.io
[22] W.S. Rasband. ImageJ Wiki [site]. URL: https://imagej.net/ij
[23] P.-E. Øren, S. Bakke, O.J. Arntzen. SPE J., **3**, 324 (1998).
[24] W. Weibull. J. Appl. Mech., **18** (3), 293 (1951).
[25] N.R. Morrow. J. Can. Pet. Technol., **14**, 1 (1975).
[26] T. Sottmann, C. Stubenrauch. *Microemulsions: background, new concepts, applications, perspectives* (Blackwell Publishing, Ltd, 2009), p. 1–47.

Translated by M.Shevelev